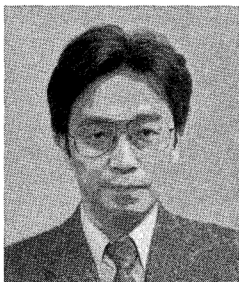
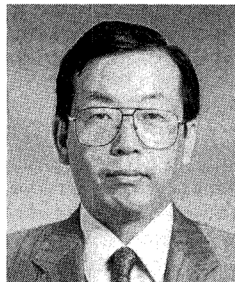


STRENGTH DEVELOPMENT MECHANISM OF PORTLAND CEMENT PASTE

(Translation from Concrete Research and Technology, Vol.5, No.1, Jan. 1994)



Takaharu GOTO



Taketo UOMOTO

The influence of curing time and water-cement ratio on hardened cement paste is investigated by both experimental and analytical methods. The compressive strength and pore size distribution of hardened pastes of Alite and ordinary Portland cement were measured in experiments. Two different models, one concerned with compressive strength development by cement hydration reaction and the other concerned with the aggregation of cement particles in cement paste, are considered. In the compressive strength development model, it is assumed that strength develops with increasing contact area between adjacent cement particles due to the hydration. In the model based on the aggregation of cement particles, it is assumed that fine cement particles aggregate first due to the influence of water cement ratio. It is found that the experimental results for pore structure and the compressive strength development of hardened cement paste agree well with calculated results based on these models.

Key words: *structure of hardened cement paste, pore structure, hydration, water-cement ratio, aggregation*

T. GOTO is a chief researcher at the Central Research Laboratory at Nihon Cement Co., Ltd, Tokyo, Japan. His research interests include cement chemistry. He is a member of JSCE and JCI.

T. UOMOTO is a professor at the Institute of Industrial Science at the University of Tokyo, Tokyo, Japan. He received his Doctor of Engineering Degree from the University of Tokyo in 1981. He specializes in composite materials for construction, such as durability of concrete, fiber-reinforced plastics and application of nondestructive testing methods for concrete structures, he is a member of JSCE, JCI, ACI and JSNDI.

1. INTRODUCTION

It is known that the structure of hardened Portland cement paste greatly affects the physical properties of concrete. Structure has a direct effect on the compressive strength of hardened cement paste. The pore structure that forms in the paste affects the durability characteristics of the hardened cement, such as permeability and carbonation. In investigating the structure of hardened cement paste, we need to consider both the structure surrounding the hydrate crystals and the structure of hydrate crystals themselves. Each hydrate has a unique crystal structure which depends on temperature. Since the structure surrounding the hydrate crystals is related to the space in which they form, factors determining the location of water and solid particles --such as water-cement ratio-- affect it significantly. Consequently, influence of water-cement ratio on the compressive strength of hardened cement paste is very significant.

So far, however, no quantitative estimation has been performed to check whether the water-cement ratio has an influence at each stage of the hydration leading to hardened Portland cement paste. The any investigations reported to date seem to concentrate on qualitative studies of the structure of hardened cement based on observations of hydrate crystals using SEM (scanning electron microscopy) and measurements of compressive strength and pore size distribution at each stage of hydration.

The purpose of this study is to explain quantitatively the influence of water-cement ratio on the structure of hardened Portland cement paste. The influence of water-cement ratio on the compressive strength and pore structure of hardened cement paste is investigated experimentally and an analytical model is proposed.

2. RELATION BETWEEN POROSITY AND COMPRESSIVE STRENGTH IN ALITE

In general, the pores in hardened cement paste can be classified as gel pores and capillary pores. Pore radii from 1nm to 3nm and 3nm to 30 μ m are called gel pores and capillary pores respectively [1]. It is believed that capillary pores affect the compressive strength of hardened cement paste significantly. However, the distinction between capillary pores and gel pores is not clear. Thus, it may be better to define capillary pores in terms of the hydration of Portland cement rather than the size of the pores in the hardened cement paste.

Since Alite, the major component of Portland cement, strongly affects the physical properties such as compressive strength, it is necessary to observe its hydration process quantitatively in order to relate porosity and compressive strength.

2.1 Calculated porosity from degree of hydration of Alite

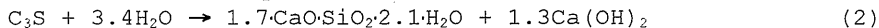
In the case of Alite, the amount of chemically bound water in C-S-H is larger than the amount of non-evaporable water retained after D-dry. The amount of bound water is nearly equal to the amount of water balanced at humidity 15% in the desorption process. The chemical composition of C-S-H in this condition is $1.7\text{CaO}\cdot\text{SiO}_2\cdot 2.1\text{H}_2\text{O}$ [2]. In the hydration of Alite, the amount of water needed for complete hydration which is greater than the amount of bound water, is approximately 42% of Alite gravity. In this case, the composition of C-S-H is supposed to be $1.7\text{CaO}\cdot\text{SiO}_2\cdot 4\text{H}_2\text{O}$ [3]. It can be considered that porosity of saturated hardened Alite may be obtained by subtracting the total amount of water from the amount of bound water in calcium

hydroxide and C-S-H which composition $1.7\text{CaO}\cdot\text{SiO}_2\cdot 4\text{H}_2\text{O}$. Then, the porosity can be calculated by measuring amount of bound water.

The amount of water needed for complete hydration of Alite:



The amount of chemically bound water:



The amount of bound water which can be measured by experiment is 3.4 mol per C_3S as in Equation (2), and the amount of water which can define the porosity is 5.3 mol per C_3S as in Equation (1). We can then calculate the amount of water (1) by multiplying 5.3/3.4 and the amount of bound water measured together.

2.2 Experimental method

Alite was synthesized by mixing raw materials of top industrial grade to match Alite composition proposed by Yamaguchi [4] and baking at $1,550^\circ\text{C}$ for 8 hours in an electric furnace. The synthesized Alite, containing 0.17% of f-CaO, was ground to achieve Blaine surface areas of 3,240; 3,950; 4,580 cm^2/g in a ball mill.

The three kinds of synthesized Alite were mixed to 40, 50, and 60% water-Alite ratio, and the resulting Alite paste was molded into $1\times 1\times 7$ cm forms. After the specimens were cured in moist conditions for one day, they were cured in water at 20°C . Compressive strength was measured after 3, 7, and 28 days of curing. Simultaneously, non-evaporable water, bound water and ignition loss at $1,000^\circ\text{C}$ were measured. The pore size distribution of samples after D-dry was measured using a mercury porosimeter (Autopore 9220 made by Micromeritics) over the range of intrusion pressure from 0.04 to 4,200 kgf/cm^2 .

2.3 Results and discussion

(1) Compressive strength and amount of bound water

The compressive strength of Alite paste was measured after 3, 7 and 28 days of curing time as mentioned above. The results are shown in Table 1. Compressive strength paste increases with curing time and with lower of water-Alite ratio (W/C). However, the compressive strength of hardened Alite paste with 4,580 cm^2/g Blaine fineness, 40% water-Alite ratio, and 4 weeks of curing seems to be lower. This may be explained as follows: the contribution of fineness to compressive strength decreases as curing progress, and also inability to form a packed structure of this paste. The maximum compressive strength observed was 867 kgf/cm^2 .

As in Table 1, the actual water-Alite ratio (W'/C) measured from hardened Alite paste seems to be lower than the water-Alite ratio (W/C) established, and separation of water from Alite increases with coarser Alite. The decrease in actual water-Alite ratio is a maximum of 7% at 60% water-Alite ratio. No difference arises at a 40% water-Alite ratio.

Table 2 shows the amount of non-evaporable water and the amount of bound water for each curing time. The amount of non-evaporable water and bound water in the Alite paste increases as curing progresses and as the Alite becomes finer, reflecting the progress of Alite hydration. However, the amount of bound water does not differ much with changing water-Alite ratio.

From this evidence, it can be considered that mole ratio of bound water (H/Ca) retained after desiccation at 15% humidity is almost constant regardless of curing time, fineness, and water-Alite ratio.

Table 1 Compressive strength of hardened Alite paste (kgf/cm²)

fineness	W/C (%)	W'/C (%)	3 days	7 days	28 days
3,240cm ² /g	60	56.2	58	100	242
	50	45.5	121	190	441
	40	37.7	288	470	867
3,950cm ² /g	60	58.1	72	120	275
	50	47.8	157	243	468
	40	39.3	365	538	867
4,580cm ² /g	60	57.3	92	140	302
	50	48.4	189	278	517
	40	39.5	457	620	757

Note) W'/C represent actual water Alite ratio.

Table 2 Amount of non-evaporable water and amount of bound water (g/g-Alite)

fineness	W/C (%)	Non-evaporable water			Bound water		
		3 days	7 days	28 days	3 days	7 days	28 days
3,240cm ² /g	60	0.116	0.147	0.169	0.163	0.196	0.248
	50	0.112	0.152	0.142	0.164	0.195	0.215
	40	0.128	0.173	0.168	0.169	0.203	0.246
3,950cm ² /g	60	0.133	0.160	0.173	0.185	0.214	0.261
	50	0.128	0.166	0.180	0.178	0.211	0.263
	40	0.133	0.172	0.179	0.181	0.212	0.263
4,580cm ² /g	60	0.130	0.158	0.176	0.191	0.216	0.270
	50	0.136	0.170	0.180	0.190	0.226	0.266
	40	0.149	0.186	0.190	0.201	0.232	0.268

(2) Calculated porosity from amount of bound water

Porosity can be calculated using equation (3) from the actual water-Alite ratio shown in Table 1 and the measured amount of bound water in Table 2. Table 3 gives the results of porosity calculated using equation (3).

Table 3 Pore volume calculated by bound water (ml/ml)

fineness	W/C (%)	3 days	7 days	28 days
3,240cm ² /g	60	0.361	0.314	0.252
	50	0.297	0.236	0.168
	40	0.199	0.135	0.038
3,950cm ² /g	60	0.341	0.289	0.225
	50	0.277	0.225	0.137
	40	0.185	0.117	0.073
4,580cm ² /g	60	0.326	0.278	0.210
	50	0.262	0.193	0.133
	40	0.146	0.080	0.014

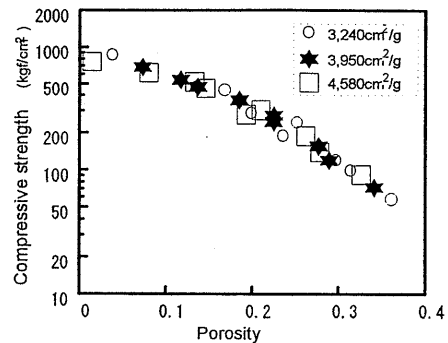


Figure 1 Porosity calculated by amount of bound water and strength

$$\text{Porosity} = W'/C - 5.3/3.4 \times \text{bound water} \quad (3)$$

Figure 1 shows relation between measured compressive strength and pore volume obtained by calculation. From this figure, it is evident that there exists a strong correlation between porosity, as calculated from the amount of bound water using the Alite hydration equation, and compressive strength.

(3) Pore size distribution measured by mercury intrusion porosimetry

Figures 2 and 3 show examples of pore size distribution for various curing times and water-Alite ratios for hardened Alite paste. From Figure 2, it can be seen that pores of size corresponding to an intrusion pressure of 1,000-4,200 kgf/cm² (pore radius: 7.5-1.8nm) are constant regardless of curing time, and that the characteristic that varies with curing time is the pore volume corresponding to intrusion pressure of less than 30kgf/cm² (pore radius above 250nm). Figure 3 shows the pore size distribution for various water-Alite ratios. Regardless of water-Alite ratio, the pore volume is constant above 500 kgf/cm² (pore radius: 15nm), but the pore volume at intrusion pressures of less than 500kgf/cm² changes significantly with water-Alite ratio.

Observations of Figures 2 and 3, demonstrate that for intrusion pressures above 1,000 kgf/cm², the water Alite ratio has a minimum effect on pore volume. Therefore, it can be concluded that there is a powerful influence only for pores of less than 1,000 kgf/cm² intrusion pressure.

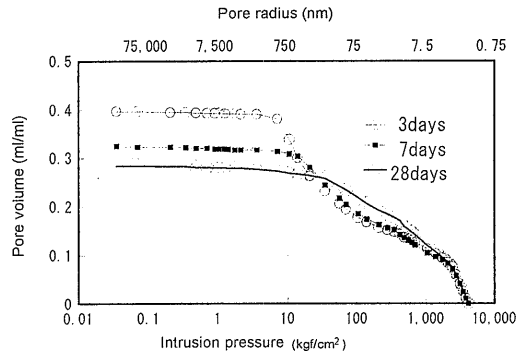


Figure 2 Example of pore size distribution for different curing times

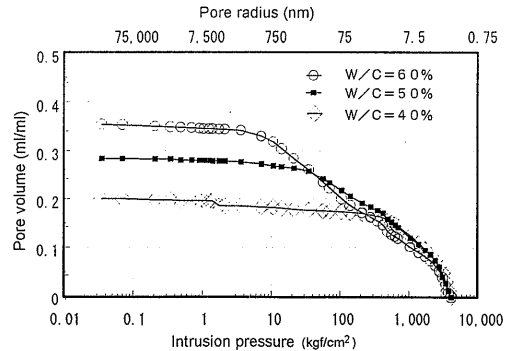


Figure 3 Example of pore size distribution for different water-Alite ratios

Table 4 Pore volume of hardened Alite paste (ml/ml)

fineness	W/C (%)	Value of intrusion pressure					
		Max=4,200kgf/cm ²			Max=1,000kgf/cm ²		
		3 days	7 days	28 days	3 days	7 days	28 days
3,240cm ² /g	60	0.457	0.391	0.366	0.360	0.285	0.258
	50	0.409	0.325	0.307	0.291	0.201	0.169
	40	0.301	0.245	0.215	0.185	0.116	0.067
3,950cm ² /g	60	0.435	0.370	0.354	0.317	0.255	0.235
	50	0.397	0.325	0.284	0.271	0.204	0.143
	40	0.304	0.215	0.200	0.171	0.089	0.056
4,580cm ² /g	60	0.421	0.379	0.334	0.301	0.256	0.216
	50	0.348	0.299	0.223	0.235	0.176	0.083
	40	0.268	0.212	0.193	0.139	0.061	0.036

Table 4 shows the total pore volume for intrusion pressures up to 4,200 and 1,000 kgf/cm² measured with a mercury porosimeter. From Tables 3 and 4, calculated pore volumes are lower approximately 0.2 ml/ml than the total pore volume for intrusion pressure up to 4,200 kgf/cm², but is almost equal in that up to 1,000kgf/cm². From this, it can be concluded that pore values corresponding to an intrusion pressures less than 1,000kgf/cm² are related to compressive strength, and thus can be considered equivalent to capillary pores.

3. Pore size distribution in hardened Portland cement paste

In hardened Alite paste, pore radii related to compressive strength are larger than 7.5nm (intrusion pressures of less than 1,000kgf/cm²). On the other hand, it is known that the pore structure has a great influence on the physical properties of concrete. Because curing time and water-cement ratio greatly affect the pore structure of hardened cement paste, the change in pore structure due to these factors was measured by mercury porosimetry. An investigation of pore structure by cement hydration reaction model was also performed.

3.1 Experimental procedure

The type of cement is ordinary Portland cement. The particle size distribution was measured using a particle size analyzer of laser diffraction type. The results are shown in Table 5. Water-cement ratios (W/C) range from 20% to 60%. For cement pastes with 20-30% water-cement ratios, 2wt% of amino-sulfuric acid superplasticizer was added. Cement pastes were mixed for 3 minutes and molded into cylinders $\phi 5 \times 10$ cm. After curing in a moist atmosphere for one day, they were cured in water for certain times. After curing, compressive strength was measured and the pore size distribution was obtained by mercury porosimetry after drying using a vacuum pump.

Table 5 Particle size distribution of ordinary Portland cement

grain size(μ m)	cumulation(%)	increment(%)
0.1	0.4	0.4
0.2	0.8	0.4
0.4	1.7	0.9
0.6	2.6	0.9
0.8	3.5	0.9
1.0	4.4	0.9
1.5	6.8	2.4
2.0	10.1	3.3
3.0	15.1	5.0
4.0	20.0	4.9
6.0	26.9	6.9
8.0	34.1	7.2
12.0	45.1	11.0
16.0	55.3	10.2
24.0	73.1	17.8
32.0	84.2	11.1
48.0	95.3	11.1
64.0	98.3	3.0
96.0	100.0	1.7

3.2 Results of experiments

(1) Pore size distribution

Figure 4 shows an example of pore size distribution for hardened cement paste (W/C =50%). It is clear that porosity and average pore radius decrease with longer curing times. A threshold pore radius can be seen in all intrusion curves, identified by the pressure at which a large quantity of mercury first penetrates.

Figures 5 and 6 show pore size distribution curves drawn for different hardened cement pastes with various water-cement ratios cured for one day. Figure 5 (hardened cement paste without the admixture) shows that the threshold radius becomes smaller with decreasing W/C at one day and is 70nm for W/C=30%. Figure 6 gives the pore size distribution of cement paste made

with the superplasticizer. The threshold radius falls with decreasing W/C, but suddenly rises to 700nm for cement paste with W/C =20%. It is thought that this threshold radius increase arises because the pore volume of hardened cement paste is greater as a result of lack of packing ability due to lower fluidity. Also, by comparing Figure 5 and 6, it is clear that when W/C=30%, the threshold radius of cement pastes with superplasticizer is larger than those without the admixture.

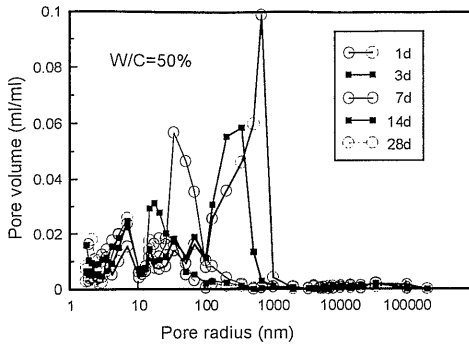


Figure 4 Pore size distribution for different curing times (W/C=50%)

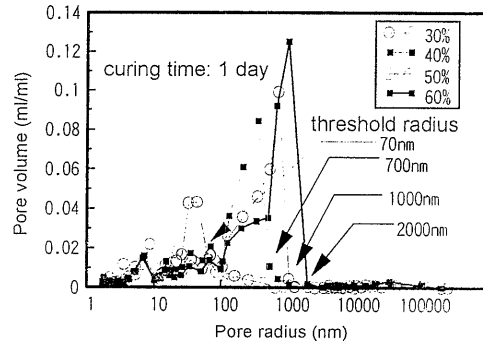


Figure 5 Pore size distribution for different of W/C values (curing time: 1 day)

(2) Compressive strength

Table 6 shows the results of compressive strength measured at curing times from 1 to 91 days with water-cement ratios (W/C) from 20 to 60% in the case of ordinary Portland cement. Usually, the actual W/C is lower than the initial W/C due to separation of water. In the case of W/C =60%, this reduction is W/C is 9%. However, in the case of W/C =20% with superplasticizer, the actual W/C is higher. This is thought to be due to an increase in pore volume caused by lack of packing ability.

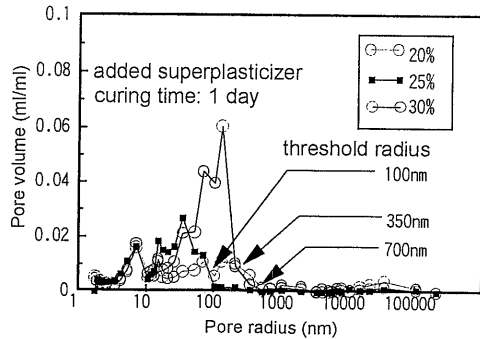


Figure 6 Pore size distribution for different W/C values (with added superplasticizer; curing time: 1 day)

Table 6 Relation between compressive strength (kgf/cm²) and actual water-cement ratio

	W/C (%)	W' / C (%)	1 day	3 days	7 days	14 days	28 days	91 days
without admixture	60	51.0	29	79	157	236	340	511
	50	44.1	47	133	259	436	552	604
	40	38.0	97	258	528	651	772	740
	30	29.3	259	505	520	541	549	469
with superplasticizer	30	29.5	88	428	743	765	1064	1107
	25	24.5	403	790	961	1115	1241	1412
	20	21.1	457	728	809	920	923	1227

W' / C is actual water-cement ratio calculated from ignition loss of sample.

3.3 Discussion

As mentioned above, the threshold radius changes with water-cement ratio. It is inconceivable that pores with a radius greater than $1\mu\text{m}$ are produced regularly by cement particles of grain size above sub-micron level (see Table 5).

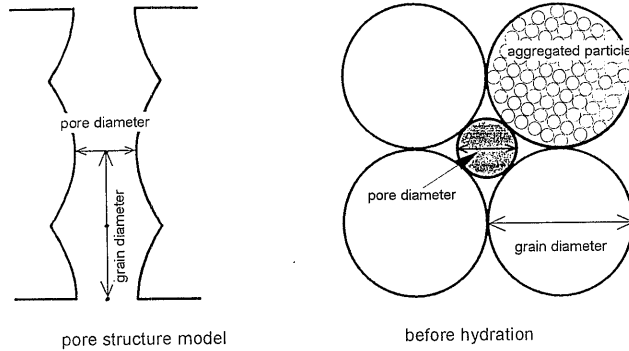


Figure 7 Concept of pore structure cubic packing arrangement

A model (see Figure 7) is proposed to explain the behavior in which threshold radius changes due to water-cement ratio, curing time, and the addition of super-plasticizer. It is assumed that a cement hydrate is formed outside the cement particles, thus forming the pore structure, when cement reacts with water. During the stage in which cement particles are in contact with each other, compressive strength development begins, and pores are regarded as osculating spheres in contact with cement particles of the same size, giving the packing arrangement shown in Figure 7. The volume fraction of cement particles in this case is $(4/3 \times \pi) / 8 = \pi / 6 = 52.3\%$, because a spherical cement particle is inscribed within a cube. The measured pore radius is the smallest possible radius in this pore model based on mercury intrusion porosimetry. Therefore, the pore radius is approximately $1/4.8$ of the grain size (diameter). By using Equation (4), the pore radius can be calculated. In this case, the relation between pore radius and grain size ($2xr$), is as follows.

$$\text{pore radius} = (\sqrt{2} - 1) \times r \quad (4)$$

The pore radius given by Equation (4) can be assumed to be the threshold radius at one day, if the initial stage of compressive strength development is at one day. For example, in the case of 60% W/C, as described above, the calculated grain size is approximately $9.6\mu\text{m}$ with a $2,000\text{nm}$ threshold radius. But, from the particle size distribution given in Table 5, it is clear that approximately 35% of particles are less than $8\mu\text{m}$, and this cannot be explained using this model.

The fine particles are assumed to aggregate as shown in Figure 7. From this assumption, the grain size of aggregated particles is similar to that of non-aggregated particles and the packing arrangement is cubic, which has the highest porosity. It is calculated as 27.4% ($=0.523 \times 0.523$) for volume fraction of aggregated particles and 52.3% for non-aggregated particles when the packing arrangement is the same. Therefore, we can quantitatively say that an increase of water-cement ratio is the increase of quantity of

aggregated particles, as actual volume of cement particles decrease when aggregation occurs. As shown in Figure 8, the relation between water-cement ratio and quantity of aggregated particles can be calculated from the packing arrangement (cubic packing arrangement : model A) and specific gravity of cement (3.15).

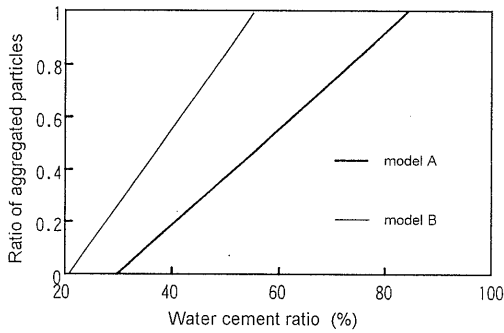


Figure 8 Relation between ratio of aggregated particles and W/C

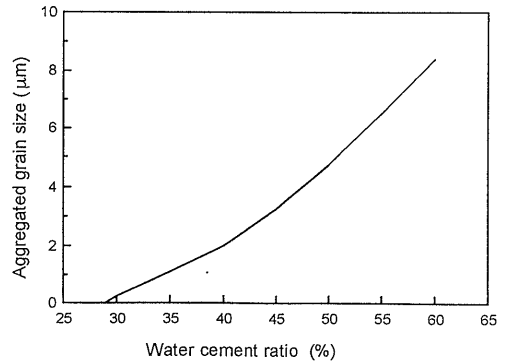


Figure 9 Relation between W/C and aggregated grain size

From the particle size distribution of the ordinary Portland cement used in this test (shown in Table 5) and the aggregation of particles occur from fine division according to this model, the relation between apparent grain size by aggregation (aggregated grain size) and water-cement ratio is obtained. Figure 9 shows this relation. Accordingly, the apparent grain size increases with water cement ratio as shown in Equation (4) and it is considered that the pore radius becomes larger as a result.

The ratio of aggregated particles can be calculated from the actual water-cement ratio, and the aggregated grain size can be obtained from the particle size which fits a cumulation value of particle size distribution of cement (shown in Table 5). Table 7 shows this result. The aggregated particle size nearly corresponds to the proportional grain size as calculated from the threshold radius.

On the contrary, the threshold radius falls if superplasticizer is added for the same water-cement ratio. The reason for this may be a change in packing arrangement due to the addition of the superplasticizer. The packing arrangement is assumed to be orthorhombic (see Figure 10) instead of cubic (see Figure 7) for cement paste with the superplasticizer. In the orthorhombic packing arrangement, the calculated volume fraction of particles is 0.605. This is larger than in the cubic arrangement. In this case, the relation between pore radius and grain size ($2xr$) is as follows.

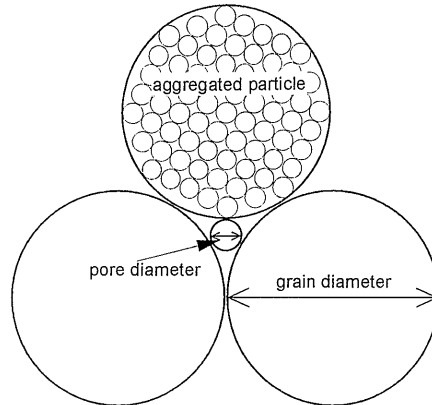


Figure 10 Packing structure with addition of superplasticizer orthorhombic packing arrangement

$$\text{Pore radius} = (2 \times \sqrt{3} - 3) / 3 \times r \quad (5)$$

Accordingly, if the grain size is the same in the cubic arrangement, the pore radius is calculated to be small with approximately 1/13 compared with 1/4.8 of Equation (4), and if the measured pore radius is the same, the proportional grain size is larger. Model B in Figure 8 shows the relation between water-cement ratio and quantity of aggregated particles in this packing arrangement, when the packing arrangement of aggregated particles assumed to be cubic. The aggregated particle size is larger, so the quantity of aggregated particles is higher when the water-cement ratio is same. For example, the proportion of aggregated particles in Model B is 38 %, while it is 4 % in Model A for the same water-cement ratio of 30%. Table 7 shows aggregated particle size as calculated by Model B. It is almost same as the proportional grain size when calculated by Model B. Due to this result, it can be considered that the threshold radius increases with the addition of superplasticizer, and this can be explained by a change in packing arrangement.

Table 7 The measured and calculated threshold pore radius (nm)

	W/C (%)	W/C (%)	Threshold radius	Proportional grain size	Aggregated particle size	
					Model A	Model B
without superplasticizer	60	51.0	2000	4800	5000	-
	50	44.1	1000	2400	3100	-
	40	38.0	700	1700	1600	-
	30	29.3	70	170	100	-
with superplasticizer	30	29.5	350	850 (2500)	100	1800
	25	24.5	100	240 (650)		850
	20	21.1	700	1700 (4500)		100

note) () is proportional grain size calculated from Model B.

4. Compressive strength development model for hardened cement paste

4.1 Basic model

Many reports on the compressive strength development of Portland cement have been published. The rate of compressive strength development and the ultimate compressive strength reacted vary for each clinker mineral. Bogue and Lerch [5] reported that C₃S exhibits the fastest strength development and the highest ultimate strength. The ultimate strength of β-C₂S is similar to that of C₃S but higher than that of C₃A and C₄AF.

Further, several researchers have investigated the relationship between clinker phase composition and strength using multiple linear regression analysis and assuming the involvement of additive action [6] [7] [8]. However, the influence of clinker mineral on strength is so complex in actual cement that the compressive strength can not be predicted from clinker phase composition alone. Reactivity and particle size distribution must also be considered as factors influencing compressive strength.

It has been said that cement strength is related to the gel-space ratio, which depends on the amount of hydrate formed [9]. Therefore, the influence

of hydration on strength development is considered to be as follows.

- (a) to increase the amount hydrate when a non-hydrated mineral reacts with water
- (b) to decrease the overall porosity due to hydration

It is difficult to analyze the first factor quantitatively, since there are various opinions about the contribution to compressive strength of each hydrate and the difference in contribution to strength of hydrated and non-hydrated mineral [10][11]. Regarding the second factor, certain equations describing the relation between strength and porosity have been proposed [12][13], and a model has been proposed that the contribution of each clinker mineral to strength is independent so that pore is filled and porosity is decreased [14]. However, the applicability of these relations between strength and porosity is limited.

Knudsen suggested that strength development in sintered ceramics is proportional to the contact area between particles [15]. We apply this concept to the cement hydration and propose a cement strength development model as follows. We assume that each spherical cement particle, which is in the center of a cube, increases in volume due to the hydration and comes into contact with the surface of the cube. Figure 11 shows an outline of this model. The ratio of outside cube to internal sphere depends on the water-cement ratio. The change in cement volume resulting from the hydration is proportional to the degree of hydration. When the hydrate comes into contact with the cube surface, it spreads out to fill the cube like a concentric sphere and the contact area on cube surface gradually increases. This contact area reflects strength development, and we assume that compressive strength is proportional to contact area. We still do not consider the type of hydrate in this case. Also, it is assumed that the strength of non-hydrate is similar to that of the hydration product.

In this model, the relation between porosity and compressive strength is unique regardless of water-cement ratio and curing time, etc. Figure 12 shows this relation. It is quite similar with the gradient of Ryshkewitch' equation for porosity less than 0.30 and the calculated gradient (b) is 5.0. The relation between compressive strength proposed by Ryshkewitch is

$$\sigma = \sigma_0 \times \exp(-b \times P) \tag{6}$$

Where, σ is compressive strength, σ_0 is the ultimate strength, and P is the porosity.

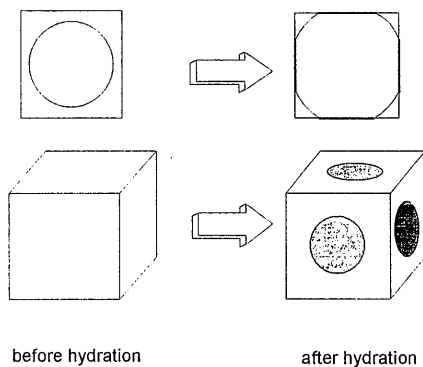


Figure 11 Concept of cement strength development model

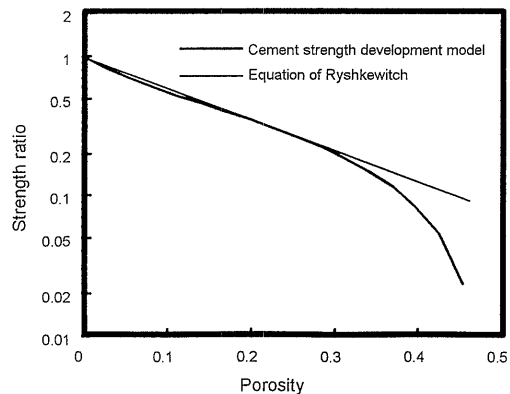


Figure 12

Relation between strength and porosity by model

4.2 Numerical formula for rate of cement hydration

A numerical formula for the hydration of Alite has been proposed by the authors [16]. In this model, it is assumed that Alite reacts uniformly toward the center of a particle, regardless of grain size, and the rate equation can be expressed as in terms of two kinds of reactions both controlled by diffusion. Figure 13 shows the analytical and experimental results of hydration rate. As shown in the figure, the reaction of Alite can be predicted by the model regardless of Alite fineness.

Since Alite contributes most to the strength of ordinary Portland cement, it can be considered that the hydration rate of ordinary Portland cement should be similar to that of Alite.

4.3 Model of water-cement ratio influence

It is assumed that all particles disperse uniformly according to the water-cement ratio. In the strength development model, which is shown in Figure 11, since the ratio of size of cube to sphere size represent the water-cement ratio, the water-cement ratio can be expressed as the function of the length of a cube side. This model expresses "uniformly dispersed model".

When the grain of the cement are of two sizes, the water-cement ratio can be expressed as a function of ratio of the two grain size, as the amount of aggregated particles increase with water cement ratio. This model expresses "aggregated particle model".

In the aggregate particle model, the hydration rate of aggregated particles is assumed to be as follows. Until the hydrate of aggregated particles fills up the space around finer aggregated particles, each one acts as an individual particles according to numerical formula for hydration rate. Afterwards, they react as apparent non-aggregated particle of the same grain size. If it is assumed that the increase in volume due to hydration is approximately 1.26 times, the space around non-hydrated particle is 0.91 ($=0.477/0.523$) times of non-hydrated particle. An aggregated particle acts as individual particle up to 0.72 ($=0.91/1.26$) degree of hydration, and afterwards it reacts as an aggregate.

5. Comparison between the model and measured strength data

Table 8 shows the relation between strength and porosity with curing time according to the uniformly dispersed model. In this case, the calculation was based on the precept that each cement particle may react toward the center of particle in same rate based on hydration rate model. Alite and cement particles are spherical and their size is 10 μm . The relation between compressive strength and porosity in this case coincides closely with that shown in Figure 12.

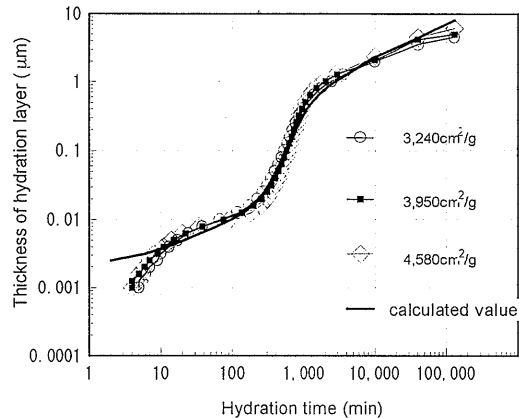


Figure 13 Hydration rate of Alite

Table 8 Relation between compressive strength and porosity obtained using the uniformly dispersed model

	W/C (%)	1 day	3 days	7 days	28 days	91 days
thickness of hydration layer(μm)	-	0.5	1.2	2.3	4.5	8.1
degree of hydration(%)	28.9	28.1	59.5	72.2	72.2	72.2
	40 \leq	28.1	59.5	86.4	99.9	100.0
compressive strength (kgf/cm ²)	28.9	240	660	1100	1100	1100
	40	90	340	680	1100	1100
	55	0	140	320	440	440
	70	0	30	160	230	230
porosity	28.9	0.291	0.084	0.000	0.000	0.000
	40	0.401	0.226	0.076	0.006	0.000
	55	0.504	0.361	0.236	0.173	0.173
	70	0.576	0.454	0.348	0.295	0.295

Table 10 shows the relation between strength and porosity in the aggregated particle model. In this case, the size of coarse and fine grains calculated as assuming 10:1 ratio of amount of coarse and fine grain and having 3200cm²/g specific surface area. Table 9 shows the relation between water-cement ratio and grain size.

Table 9 Relation between water cement-ratio and ratio of coarse and fine grains

water cement ratio(%)		40	55	70
coarse grain	grain size(μm)	23.40	40.20	51.40
	ratio (%)	67	36	15
fine grain	grain size(μm)	2.34	4.02	5.14
	ratio (%)	33	64	85

Table 10 Relation between compressive strength and porosity obtained by using the aggregated particle model

	W/C (%)	1 day	3 days	7 days	28 days	91 days
thickness of hydration layer (μm)	-	0.5	1.2	2.3	4.5	8.1
degree of hydration(%)	40	32.9	45.4	60.8	82.9	97.8
	55	39.5	55.6	62.9	74.8	88.5
	70	41.5	66.7	71.0	78.3	87.6
compressive strength(kgf/cm ²)	40	70	170	340	800	1010
	55	20	60	120	230	470
	70	7	30	50	100	200
porosity	40	0.417	0.339	0.244	0.111	0.013
	55	0.491	0.424	0.384	0.318	0.241
	70	0.542	0.452	0.431	0.396	0.353

Figure 14 shows the relations between strength and porosity for these models. The strength according to the aggregated particle model is calculated higher than the other model at low porosity.

Subsequently, Table 11 compares values calculated by this model and the compressive strength of Alite paste (Table 1). The strength of Alite compared between the measured strength at water-Alite ratio of 60% and 40% and calculated value by model of 55% and 40%, because actual value of water-cement ratio of 60 % with 3,240 cm²/g as shown in Table 1 is 56.2 %. Figure 15 shows the relation between strength and curing time. In the uniformly dispersed model, even if the surface area is small (approximately 2,000 cm²/g) because the grain size is set at 10 μm , the calculated strength is higher than the

measured compressive strength. However it is shown that the strength calculated by the aggregated particle model coincides nearly with the experimental value. This demonstrates that effect of water-cement ratio on strength may be evaluated more accurate by the aggregated particle model than by the uniformly dispersed model.

Table 11 Comparison of calculated values by models and experimental values (kgf/cm^2)

W/C	55%			40%			
	curing time	3 days	7 days	28 days	3 days	7 days	28 days
experimental		58	100	242	288	470	867
uniformly dispersed model		140	320	440	340	680	1080
aggregated particle model		60	120	230	170	340	800

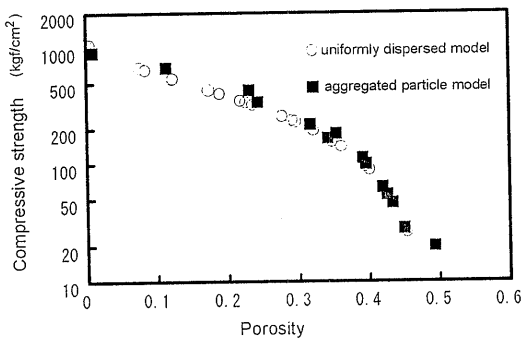


Figure 14 Relation between compressive strength and porosity by model

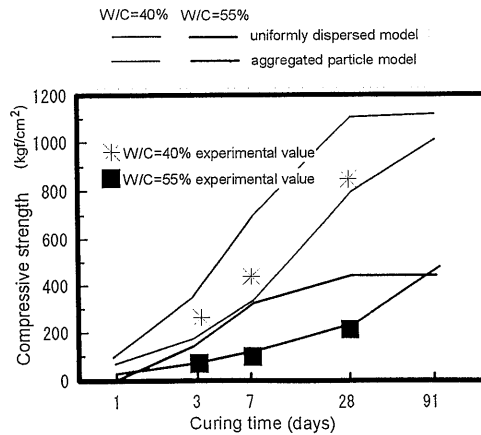


Figure 15 Compressive strength calculated models

6. Conclusion

In this paper, the influence of curing time and water-cement ratio on the strength of hardened Portland cement paste was studied through experiment and using analytical models. The results are as follows.

- 1) In the case of Alite, the porosity related to compressive strength corresponds to the porosity calculated from amount of bound water on the basis of the hydration equation.
- 2) The pore related to compressive strength is less than 1000kgf/cm^2 in intrusion pressure using mercury porosimetry (pore radius: above 7.5nm) in the case of Alite.
- 3) The aggregated particle model can explain variations in pore structure at the early stage for different water-cement ratios.
- 4) The aggregated particle model demonstrates that the packing arrangement of cement particles when superplasticizer is added is different from that with no addition.
- 5) The proposed model can explain the relation between the strength of hardened cement and the pore structure. This model combines the strength development model based on contact area between cement hydrate particle, the aggregated particle model, and the hydration formula of Alite.

References

- [1] Uchikawa H., Uchida S., and Hanehara S., *il Cemento*, Vol.88, pp.67-90, 1990
- [2] Young J.F., and Hansen W., *Mater.Res.Soc.Symp.Proc.* 85, p.313, 1987
- [3] Taylor H.F.W., *Mater.Sci.Monogr.*28A, p.39, 1985
- [4] Yamaguchi G., and Takagi S., *Proceedings of the 5th International Symposium on the Chemistry of Cement*, Tokyo 1968, Vol. I, p.181, 1969
- [5] Bouge R.H., and Lerch W., *Ind.Engng Chem.*, Vol.28, No.8, pp.837- 847, 1934
- [6] Alexander K.M., *Cem.Concr.Res.*, Vol.2, pp.666-680, 1972
- [7] Knofel D., *Zement-Kalk-Gips*, Vol.25, pp.426-431, 1978
- [8] Aldridge L.P., *Proceedings of 7th ICC*, Paris, Vol.3, pp.VI 83-86, 1980
- [9] Powers T.C., *J. Amer.Ceram.Soc.*, Vol.41, pp.1-6, 1958
- [10] Grudemo A., *Cem.Concr.Res.*, Vol.9, p.19, 1979
- [11] Lawrence C.D., *Proceedings of International Symposium, Prague*, Vol.V, p.D-167, 1973
- [12] Schiller K.K., *Nature*, Vol.180, pp.862-863, 1957
- [13] Ryshkewitch E., *J.Amer.Ceram.Soc.*, Vol.36, pp.65-68, 1953
- [14] Jons E.S., and Osbaeck B., *Cem. Concr. Res.*, Vol.12, pp.167-178, 1982
- [15] Knudsen F.P., *J.Amer.Ceram.Soc.*, Vol.42, No.8, p.376, 1959
- [16] Goto T., and Uomoto T., *47th Annual Meeting of JCA*, pp.44-49, 1993
(in Japanese)